Fabrication of Composite Hollow Fibers for Air Separation

TAI-SHUNG CHUNG,[1,*] E. RONALD KAFCHINSKI,[2] RACHEL S. KOHN,[2] PAUL FOLEY,[2] and RITCHIE S. STRAFF[2]

[1]Aeroquip Technology Center, 2323 Green Road, Ann Arbor, Michigan 48105; [2]Hoechst Celanese Research Division, 86 Morris Avenue, Summit, New Jersey 07961

SYNOPSIS

By using microporous polyacrylonitrile (PAN) hollow fibers as the substrate, we developed two types of composite fibers for air-separation. One was a poly(4-vinyl pyridine) (4-PVP)/(hexafluoro propane dianhydride)-durene(6FDA)/PAN composite hollow fiber, and the other was a 6FDA-3,5-diaminobenzonitrile/6FDA-durene/PAN composite hollow fiber. The asymmetric PAN fiber was prepared using dry-jet wet-spinning technology, and the deposition of a thin gutter layer of 6FDA-durene on PAN was carried out by prewetting PAN fibers with Fluorinert® before solution coating. The topcoating of a thin layer (200–300 Å) of PVP or 6FDA-3,5-diaminobenzonitrile on PAN/6FDA-durene fibers was conducted using a conventional solution coating method. The selectivity of 0.7% 4-PVP/2% 6F-durene/PAN composite fibers for O_2/N_2 was 5.6 with an O_2 permeance of 32.2×10^{-6} cc(STP)/cm^2 s cmHg, whereas the selectivity of 0.5% 6FDA-3,5-diaminobenzonitrile/2% 6F-durene/PAN fibers was 5.1 with an O_2 permeance greater than 37.2×10^{-6} cc(STP)/cm^2 s cmHg. Both fiber selectivities can be further improved by increasing the thicknesses of the selective layer. © 1994 John Wiley & Sons, Inc.

INTRODUCTION

Perhaps one can classify composite membranes into three categories: asymmetric composite, microporous composite, and matrix composite. Permea's polysulfone (PS) hollow fiber is a typical example of an asymmetric composite.[1-3] It consists of a low-defect asymmetric PS fiber (surface porosity $\ll 10^{-4}$) and a silicone topcoating. The silicone coating plugs the defects, while the asymmetric PS fiber determines the membrane separation performance. This method has been practiced extensively both in industry and academia to prepare defect-free membranes and to evaluate membrane performance. However, silicone coating is a secondary operation and silicone curing is a time-consuming process. Peinemann and Pinnau eliminated this problem by replacing silicone with cellulose acetate or similar materials in their poly(ether sulfone) (PES) composite membranes for separating the CO_2/CH_4 mixture.[4] The uniqueness of their idea was to seal fiber defects and to improve fiber-separation performance simultaneously by precipitating the as-spun PES fiber in a coagulation bath containing a low concentration of cellulose acetate. In case of a defect-free asymmetric as-spun hollow fiber, Chung et al. demonstrated that its separation performance can be further improved using the asymmetric composite concept by applying an additional coating of a highly selective material.[5]

As pointed out by Pinnau and Koros,[6] the separation performance of a defect-free integrally skinned asymmetric membrane would be reduced if there is a resistance in its own substructure. Therefore, a new generation membrane must consist of an ultrathin skin layer (thickness < 1000 Å) and a very porous substructure. Fabrication of an asymmetric fiber with such structure is not an easy task, but it can be done if one uses a microporous composite approach. Basically, a microporous composite membrane consists of at least a thin selective layer backed by a microporous substrate. The substrate structure may be either asymmetric or symmetric, but its surface is full of submicron pores and gases transport through it by means of Knudsen diffusion or convective flow. The main purposes of this support layer are to eliminate substantial substructure resistance of gas transportation and to provide

* To whom correspondence should be addressed.

Journal of Applied Polymer Science, Vol. 53, 701–708 (1994)
 CCC 0021-8995/94/050701-08

membranes with reasonable mechanical properties such as compression strength and collapse pressure. Cadotte's FT-30 desalination membrane is an example of a microporous composite membrane where he induced an interfacial polycondensation reaction on the surface of a microporous PS membrane.[7] The air-separation and pervaporation membranes developed by Kimmerle et al.[8] and Gudernatsch et al.[9] are good examples of microporous composites where they coated a defect-free poly(dimethyl siloxane) (PDMS) or poly(butadiene styrene) (BS) layer on the inner surface of a microporous poly(ether sulfone) (PES) hollow fiber.

A mathematical model for gas diffusion through these membranes has been proposed by Pinnau et al.[10] Niwa et al.[11] employed the same concept and developed glass/ceramic composite membranes for separating CO_2 and CH_4. Basically, they deposited a thin glass membrane (5–23 μm thick) on a porous ceramic tubing. The mean pore diameter of their membrane was 4–64 nm. However, the gas absorption, diffusion, and separation mechanisms for polymeric composite membrane and glass/ceramic membranes may be quite different.

The matrix composite membrane is made using a mixture of polymers as the selective layer on a microporous support or by forming the mixture as an asymmetric membrane. Much work has been done by Paul and co-workers to define the separation performance of miscible blends.[12,13] By controlling the blend composition, one can easily select a blend with a specific separation performance. Kajiyama et al. developed ternary composite membranes based on a poly(vinyl chloride)/liquid crystal/fluorocarbon formulation.[14] Researchers at Texaco invented a matrix composite of a poly(vinyl alcohol) (PVA) and a poly(acrylic acid) on a microporous polyacrylonitrile (PAN) support for the separation of organic liquids.[15] Compared to the development of asymmetric composites and microporous composites, the matrix composite membranes are in the early development stage.

At present, most commercial products for air-separation are derived from the asymmetric composite concept. This is because the fabrication of asymmetric membranes is generally well known, raw materials have reasonable air-separation performance, and their costs are relatively low. However, fabrication of an asymmetric membrane is no longer cost-effective if an expensive polymer is used. In addition, since the requirements for the degree of perfection for air-separation membranes are much greater than for reverse osmosis (RO), it is sometimes difficult to form a useful asymmetric membrane from a brittle polymer. One must adopt the multilayer microporous composite concept to fabricate membranes from these expensive or brittle polymers. Not only does it reduce material quantities and costs, but it also produces membranes having maximum benefit from their unique separation performance. Therefore, much effort was spent to develop new-generation air-separation membranes based on the multilayer microporous composite concept. Cabasso and Tamvakis developed polyethyleneimine/PS hollow fibers for RO and found that the PS substrate must have surface pore diameters of less than 0.2 μm to obtain useful performance.[16] They manipulated surface pore size by heat-treating microporous PS fibers at 110–150°C for less than 30 min. Bikson et al. at Union Carbide extended and modified Cabasso and Tamvakis' approach and developed various composite membranes for H_2/N_2 separation.[17] They first converted a microporous, nonasymmetric PS hollow fiber to a slightly selective asymmetric hollow fiber by annealing at about 182°C for 10 s before the deposition of a selective layer.

Using poly[1-trimethyl(silyl)-1-propyne] (TMSP) to form a microporous composite membrane was reported by Air Products.[18] This membrane performance can be further improved by plasma or fluorooxidation treatment.[19,20] As a result, TMSP became an intermediate layer between the selective layer (surface-modified layer) and the microporous substrate. Generally, the intermediate layer in a composite membrane is referred to as the gutter layer and is usually made of a highly permeable material. The purpose of this layer is to enhance the adhesion between the top layer and the substrate and to improve the permeance through this multilayer membrane. A composite membrane may have multiple gutter layers as demonstrated by Bruschke.[21]

In this article, we report the performance of various composite fibers based on microporous PAN substrates and reveal a new method to deposit a thin gutter layer on nonselective microporous PAN hollow fibers. PAN fibers have been used extensively as the substrate for various composite membranes.[15,22] This is because it is a low-cost material with good chemical resistance and can be easily fabricated. Takao[22] and Albrecht et al.[23] developed the basic technology for forming microporous PAN hollow fibers. An aromatic polyimide is used as the gutter-layer material; it has a high permeability with a reasonable selectivity. The top-layer materials are poly(4-vinyl pyridine) (PVP) and 6FDA–3,5-diaminobenzonitrile; they both have high selectivity. Koros et al.'s[24] and Robeson's[25] work indicated that some fluoro-containing aromatic polyimides have

excellent potential to be used in gas-separation applications.

EXPERIMENTAL

Microporous PAN Hollow Fibers

PAN material was purchased from Monsanto and the spinning dope was prepared by dispersing PAN powder in chilled *N*-methylpyrrolidone (NMP) and then heating it up to 95–100°C with continuous mixing until it was completely dissolved. The PAN content in the spinning dope varied from 20 to 24 wt % and was preferably 23–24 wt %. A 24 wt %, PAN dope had a viscosity of 650 poises at 30°C, 1080 poises at 40°C, and 720 poises at 50°C.

The o.d. and i.d. of the spinneret for spinning were 838 and 711 μm (33 and 28 mil), respectively. The outer coagulant was water and its temperature was controlled ±1°C by a Neslab temperature bath. A bore fluid, metered by an Isco® syringe pump (Model 500D), was injected into the as-spun nascent hollow fiber in order to support fiber roundness and to induce phase separation. Once the wet hollow PAN fiber emerged from the coagulation bath, it passed through a solvent exchanger to reduce residual NMP and then was dried on a roller to yield an almost solvent-free dry fiber. A detailed description of spinning equipment and the concept of dope preparation was given in a previous article.[26]

6FDA–Durene Gutter Layer

6FDA–durene polyimide was synthesized from hexafluoropropane dianhydride (6FDA) and durene diamine as previously described.[5,27] Basically, there were three steps: First, a polyamic acid was synthesized using a solution polycondensation reaction from 50 mol % 2,2′-bis(3,4′-dicarboxyphenyl) hexafluoro propane dianhydride (6FDA) and 50 mol % 3,6-durene diamine. Then, it was imidized by adding acetic anhydride and beta picoline to the solution. Finally, solid 6FDA–durene polyimide powder was obtained by precipitating the imidized solution in methanol and drying overnight in a vacuum oven at 60–65°C. The inherent separation properties of this 6FDA–durene polyimide have been measured from a dense film. Its oxygen permeability is 72 barrers and α for O_2/N_2 is about 4.3 at 25°C. Tubular glass coaters were designed for the prewetting of an as-spun dry PAN fiber with Fluorinert® 72 and for the deposition of a thin 6F–durene layer. Internally, the glass coater has a cone-shaped funnel with an i.d. of 700–750 μm. As shown in Figure 1, the PAN fiber traveled 6 M/min vertically upward through the first coating section comprising a prewetting coater, a solution coater, and a drying column. In the prewetting coater, a perfluoroether mixture, Fluorinert® 72 from 3M, was applied to the PAN fiber at a flow rate of 0.12 cc/min. Then, the fiber passed through the solution coater where a solution of 6FDA–durene in chloroform was applied to the prewetted fiber. The column temperature was set at 70°C because the boiling point of Fluorinert® 72 was 56°C.

PVP and 6FDA–3,5-Diaminobenzonitrile (6FDA–DBN) Selective Layers

A PVP/MeOH solution (Reilline® 4200) was purchased from Reilly Industries. PVP has been known to be a good barrier material, but its true separation properties are not available in the literature because it cannot be formed into a free-standing film.

The 6FDA–DBN polyimide was synthesized from 6FDA and 3,5-diaminobenzonitrile using a similar route to that of 6FDA–durene. Its oxygen permeability was 3.25 barrers, and α for O_2/N_2 was about 7.15 at 24°C.

The procedure of depositing PVP or 6FDA–DBN over the dry 6FDA–durene layer was essentially the same as was followed in the first-coating section. However, many experimental results indicated that prewetting the fiber in this stage was not important because the 6FDA–durene layer was almost defect-free.

Module Fabrication and Tests

Six centimeter single-filament short modules and 14 cm five-filament glass modules were fabricated to test PAN fiber performance. For a 6 cm five-filament module, tests were conducted by placing it in a test cell filled with either pure oxygen or nitrogen at room temperature (25°C). The test cell design was similar to that of the previous work.[10] Since PAN substrate is a microporous membrane, one can measure gas flow rates at a specific pressure and O_2/N_2 selectivity if Knudsen diffusion occurs. For composite fibers, the modules were 20 cm long with an i.d. of 1.5 cm. Each module consisted of 25–100 filaments. For both 14 and 20 cm-long glass modules, gas-flow tests were carried out by applying pressure from the shell side and the permeances were measured from the bore. The selectivity, α, for gas a to gas b is defined as

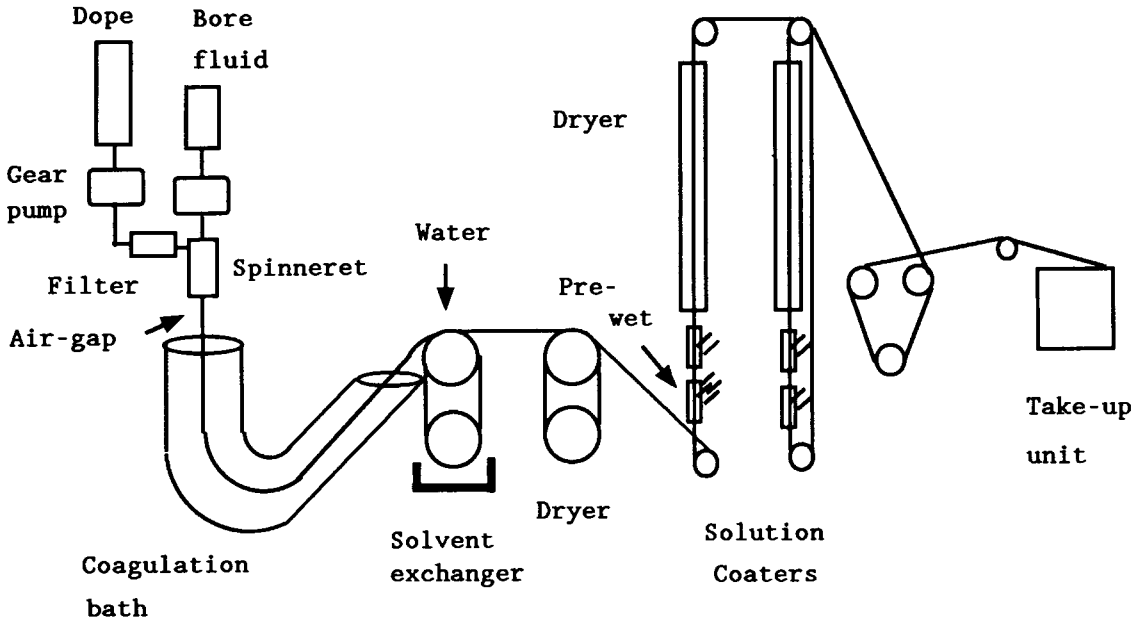

Figure 1 Schematic diagram of spinning and coating devices.

$$\alpha = \frac{\left(\frac{P}{L}\right)_a}{\left(\frac{P}{L}\right)_b}$$

where P/L is the permeance for gas a or gas b. The test temperature was about 25°C, and the pressure varied from 2 to 50 psi.

RESULTS AND DISCUSSION

Microporous PAN Hollow Fibers

Various bore fluids, such as 80/20 H_2O/NMP, 95/5 glycerine/NMP, 80/20 glycerine/NMP, and glycerine, were tried in order to create proper fiber morphology, but all failed. This was because these solvents induced fast coagulation and resulted in fibers with two dense layers located at both the inner and outer surfaces. Their overall structures across the membrane were very tight. Their air-flux rates were too low compared to that of Celgard® microporous polypropylene fiber.

Excellent morphology was obtained if NMP or 95/5 NMP/water was employed as the inner coagulant. The inner dense layer was fully destroyed and finger voids were uniformly distributed across the cross section as shown in Figures 2 and 3. Table I summarizes the air-flow rate (permeation rate) and mechanical properties of PAN fibers as a function of the percent solids in the spinning dope. An increase in the dope solids percentage resulted in an increase in the fiber maximum load (tensile stress), but it reduced the air-permeation rate because the fiber structure was getting tight. Since a melt-spinning process produces fibers with better chain entanglement and fewer microdefects than that of a dry-jet wet-spinning process, Celgard fiber has better mechanical properties than those of PAN fiber. Table II shows the effect of coagulation temperature on the fiber air-flow rate. The higher the bath temperature, the greater the flow rate. Compared to

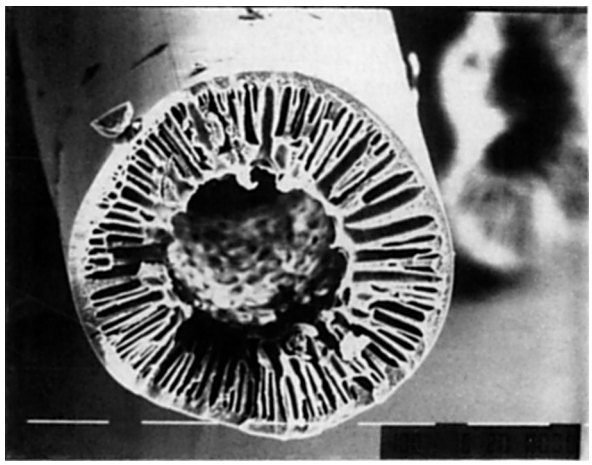

Figure 2 Cross-section view of a PAN fiber spun from a 23 wt % solid (×200).

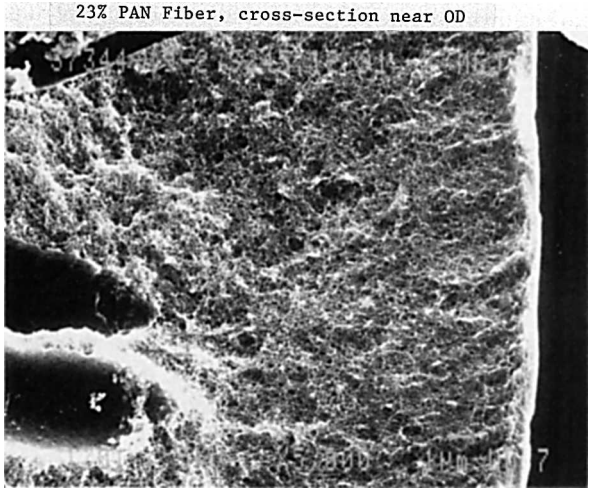

Figure 3 Cross-section morphology near the external surface of a PAN fiber spun from a 23 wt % solid (×5000).

Celgard, the newly developed PAN fiber is much more permeable if the bath temperature is 40°C or higher. As shown in Figure 4, its external surface pore size is about 150–200 Å, which is also much smaller than that of Celgard. Figure 5 illustrates the PAN fiber's internal surface structure and shows that it is fully porous.

The 95/5 NMP/water mixture was the preferred formulation as the bore fluid. It was better than pure NMP because the small amount of water induced slight coagulation and improved the stability of the spinning process.

6FDA–Durene/PAN Composite Fiber

As described in the previous section, the deposition of a thin 6FDA–durene layer on PAN was carried out by prewetting a PAN fiber with Fluorinert. The advantage of using Fluorinert is that it has a low surface contact angle; it can spread on the microporous surface of PAN fibers easily and temporarily fill the pores. As a result, the prewetting of PAN fiber with Fluorinert can prevent the solution of 6FDA–durene in chloroform solution from penetrating into the PAN fibers. As described in Cabasso and Tamvakis' work, they observed intrusion of the polymeric solution into pores to a depth as great as 2 μm. As a result, they contracted surface pore sizes and reduced intrusion by annealing the substrate. Table III summarizes the performance of PAN fibers coated with 1 and 2% solutions of 6FDA–durene. The separation performance of 1% 6F–durene/PAN fibers was very impressive; it had a permeance greater than 100×10^{-6} cc(STP)/cm^2 s cmHg with a reasonable α. For a 2% 6FDA–durene coating, the apparent 6FDA–durene thickness based on permeance was about 1.03–1.3 μm, whereas the actual coating thickness based on mass balance was about

Table I Air Flow Rate and Mechanical Properties of PAN and Celgard Fibers (Bath Temperature at 40°C)

i.d.	Air-flow Rate[a] (cc/min at 15 psi)	Max. Load[b] (g)
PAN from 20% solid	119	78
PAN from 23% solid	95	96
PAN from 24% solid	70	105
Celgard	47	230

[a] Sample length is 6 cm.
[b] Bore fluid is 95/5 NMP/H_2O.

Table II The Effect of Bath Temperature on the Air-Flow Rate of PAN Fibers (24% Solid, 85 mm Air Gap, Bore Fluid was 95/5 NMP/H_2O with a Flow Rate of 0.54 cc/min)

Bath Temp. (°C)	Air-flow Rate[a] (cc/min at 15 psi)
60	155
50	110
40	70
30	8

[a] Sample length was 6 cm.

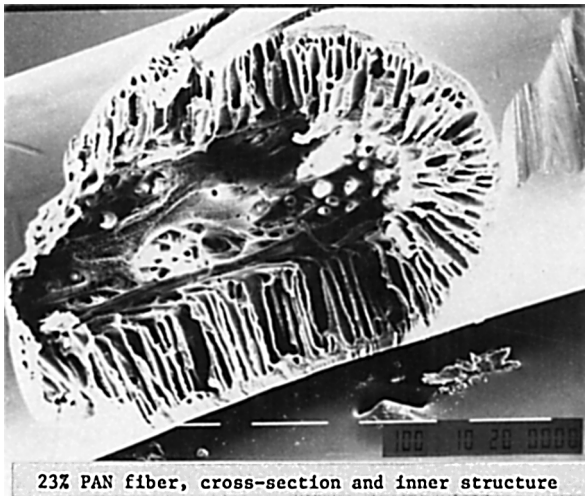

Figure 4 Internal and fracture structure of a PAN fiber spun from a 23 wt % solid (×150).

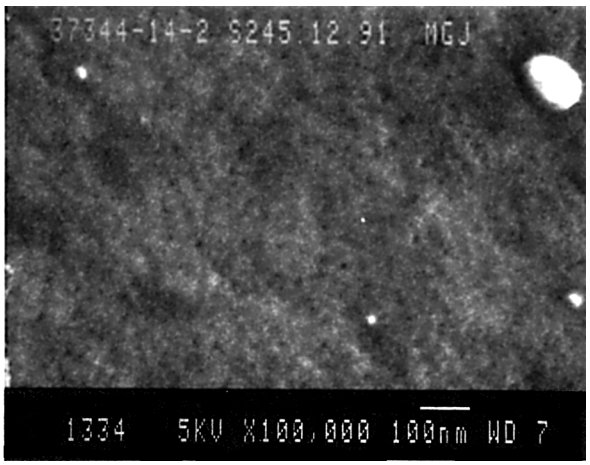

Figure 5 External surface of a PAN fiber spun from a 23 wt % solid (×100,000).

1.0 micron. If there was no prewetting agent, the apparent thickness was greatly increased due to the intrusion of the 6FDA–durene/chloroform solution. This phenomenon can be simply explained by the resistance model.[1] Figure 6 illustrates a simplified 6FDA–durene/PAN fiber cross section where layer 1 is the 6FDA–durene and layer 2 consists of two materials: One is PAN and the other is 6FDA–durene intrusion. The total flux, Q, for a component i passing through this composite membrane is

$$Q = \Delta P \left(\frac{l_1}{P_1 A} + \frac{l_2}{P_2 A_2 + P_1 A_1} \right) - 1 \qquad (1)$$

where ΔP is the total partial pressure difference across the composite membrane for gas i. P_1 and P_2 are the permeabilities of 6FDA–durene and PAN materials, respectively. A is the total fiber surface area, and A_1 and A_2 are surface areas occupied by the effective surface porosity (intruded 6FDA–durene) and the dense PAN substrate, respectively (as illustrated in Fig. 6). Since A is the sum of A_1 and A_2, eq. (1) can be rearranged as

$$\frac{Q}{A\Delta P} = \frac{P}{l} = \left(\frac{l_1}{P_1} + \frac{l_2}{P_2(A_2/A) + P_1(A_1/A)} \right) - 1 \qquad (2)$$

For a microporous PAN fiber coated with a thin 6FDA–durene layer, P_1 (72 barrers in the case of O_2) is much greater than P_2 (< 0.001 barrer) so that $P_1(A_1/A) \gg P_2(A_2/A)$. If the surface porosity of the PAN fiber is greater than 1–2%, eq. (2) becomes

$$\frac{P}{l} = \frac{P_1}{l_1} \left(1 + \frac{I_2}{l_1(A_1/A)} \right) - 1 \qquad (3)$$

As a result, the apparent permeance decreases with an increase in intrusion depth. This phenomenon is significantly enhanced if the surface porosity ratio, A_1/A, is reduced or the intrusion depth is increased. For example, $P/l = 0.2(P_1/l_1)$ if $l_1 = l_2$ and $A_1/A = 0.25$, whereas $P/l = 0.11(P_1/l_1)$ if $l_1 = 0.5l_2$ and $A_1/A = 0.25$. In other words, when a 1 μm 6FDA–durene layer was deposited on a microporous PAN fiber, the apparent thickness of this 6FDA–durene layer was about 5 μm if the intrusion would have been 1 μm. The 6FDA–durene layer would appear as a 9 μm-thick membrane if the intrusion was 2 μm. The intrusion of a polymer into surface pores limits the diffusion channels and prolongs the diffusion distance; as a result, some areas of the 6FDA–durene layer will not be fully effectively used. Although selectivity does not change, the permeance has been significantly reduced. Therefore, prewetting a microporous substrate before additional coating is a very important step to make a useful composite membrane. As shown in Table III, the perme-

Table III 6FDA–Durene/PAN Performance (20–100 Filaments Tested at 20 psi)

6FDA–Durene Concentration	Prewetting	α	O_2 Permeance (GPU[a])	Deposited[b] Thickness (μm)	Calculated[c] Thickness (μm)
1%	Yes	3.2–3.4	101.6–132.8	0.25	0.54–0.71
2%	Yes	4.0–4.3	70.4–59.6	0.99	1.0–1.21
2%	No	4.2	6.20	0.8	12

[a] 1 GPU unit = 10^{-6} cc(STP)/cm^2 s cmHg.
[b] Calculated from mass balance.
[c] Calculated from permeance.

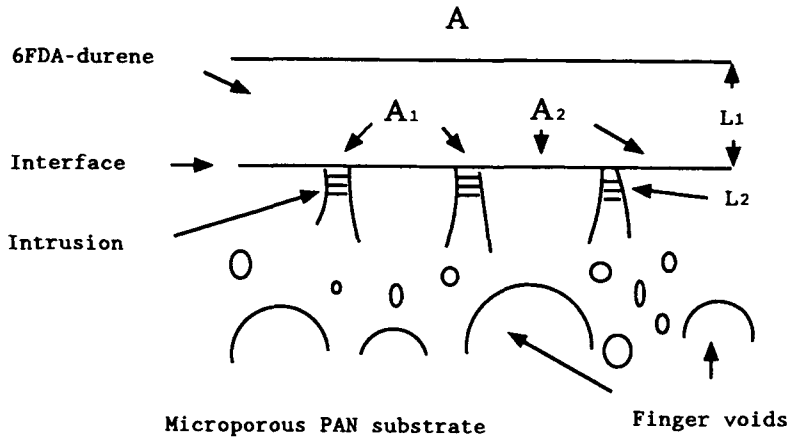

A = Surface area of a 6FDA-durene coated fiber

A_1 = Area of effective surface pores on a PAN fiber

A_2 = Area of non-porous PAN fiber surface

L_1 = Applied thickness of 6FDA-durene coating

L_2 = Depth of pore intrusion by 6FDA-durene polymer

Figure 6 Intrusion phenomenon in a composite membrane.

ance loss due to intrusion was significantly reduced when Fluorinert was used as the prewetting agent.

6FDA–DBN or 4-PVP/6FDA–Durene/PAN Composite Fibers

Table IV shows the data for composite membranes prepared using a 0.5 or 0.7% 6FDA–DBN solution applied to a 6FDA–durene/PAN composite fiber. The coating thicknesses for 0.5 and 0.7% 6FDA–DBN on 6FDA–durene were about 340 and 757 Å, respectively. The 6FDA–DBN fiber coated with a 0.5% 6FDA–DBN solution had an impressive performance; its α was 5.1 with an O_2 permeance greater than 37.0×10^{-6} cc(STP)/cm^2 s cmHg. The α increased to 5.9 and the O_2 permeance decreased to 26.7×10^{-6} cc(STP)/cm^2 s cmHg when a 0.7% 6FDA–DBN solution was used. Since the separation performances of 6FDA–DBN and 6FDA–durene were available and their coating thicknesses were known, the performances of these two 3,5-diaminobenzonitrile/6FDA–durene/PAN composite fibers were shown to be in agreement with the theoretical calculations based on the resistance model.

Table V describes the effect of prewetting the 6FDA–durene gutter layer before coating with the selective 6FDA–DBN. The data clearly indicate that the second prewetting is unnecessary if the highly permeable gutter layer is almost defect-free and the top layer is a good barrier material. As shown in the

Table IV PAN/2% 6FDA–Durene/6FDA–3,5-DBN Fiber Performance (100 Filaments Tested at 20 psi)

6FDA–DBN[a] Concentration	α O_2/N_2	O_2 Permeance (GPU[b])
0.5%	5.1	37.2
0.7%	5.9	26.7

[a] No second prewetting.
[b] 1 GPU unit = 10^{-6} cc(STP)/cm^2 s cmHg.

Table V Effect of the Second Fluorinert Wetting on PAN/2% 6FDA–Durene/0.5% 6FDA–3,5-DBN Fiber Performance (100 Filaments Tested at 20 psi)

Second Prewetting	α O_2/N_2	O_2 Permeance (GPU[a])
Yes	5.14	37.2
No	5.10	37.7

[a] 1 GPU unit = 10^{-6} cc(STP)/cm^2 s cmHg.

Table VI PAN/2% 6FDA–Durene/PVP Fiber Performance (25 Filaments Tested at 20 psi)

PVP[a] % in MeOH	α O_2/N_2	O_2 Permeance (GPU[b])
0.25	4.1	53.1
0.5	5.0	39.7
0.7	5.6	32.2

[a] No second prewetting.
[b] 1 GPU unit = 10^{-6} cc(STP)/cm^2 s cmHg.

table, the effect of intrusion by 6FDA–DBN on fiber performance is negligible. This observation is consistent with our expectation from the resistance model.

Various solutions of PVP in MeOH with a range of concentrations were prepared and deposited on 6FDA–durene/PAN fibers. As shown in Table VI, coating with 0.5–0.7% PVP results in composite fibers with impressive performance. Based on the mass balance of the PVP flow rate from the syringe pump, fiber take-up speed, and fiber o.d., one can calculate that the 0.5 and 0.7% PVP coatings have thicknesses of about 175 and 277 Å, respectively. Although PVP separation performance has never been reported and the 6FDA–durene layer may vary from 1.03 to 1.3 μm, one can roughly calculate PVP permeability at about 1.5–2.5 barrers with a selectivity for O_2/N_2 of about 6.9–7.5.

CONCLUSION

In this report, we described the fabrication of microporous polyacrylonitrile (PAN) fibers and employed them as substrates to form composite membranes. The effect of intrusion on membrane performance was thoroughly investigated, and a technique was demonstrated to reduce its effect during the fabrication of a composite hollow fiber membrane. Two interesting composite membranes were prepared using 6FDA–durene as the gutter layer and the selective layer was made of either poly(4-vinyl pyridine) (PVP) or 6FDA-3,5-diaminobenzonitrile.

Each composite fiber had an impressive separation performance with selectivity greater than 5.0 and O_2 permeance greater than 25.0 $\times$ 10^{-6} cc(STP)/cm^2 s cmHg. The dense layer thickness varied from 175 to 760 Å. Selectivity of either fiber can be further improved if the thickness of the selective layer is increased.

The prewetting technique was first suggested by Drs. C. G. Wensley, J. S. Chiou, and M. W. Tang at Separex. The authors thank them and Drs. W. M. Cooper, and R. S. Jones for providing helpful comments and discussion.

REFERENCES

1. J. M. S. Henis and M. K. Tripodi, *J. Membr. Sci.*, **8,** 233 (1981).
2. R. E. Kesting, A. K. Fritzsche, M. K. Murphy, A. C. Handermann, C. A. Cruse, and R. F. Malon, U.S. Pat. 4,871,494 (1989).
3. A. K. Fritzsche, M. K. Murphy, C. A. Cruse, R. F. Malon, and R. E. Kesting, *Gas Separation Purification,* **3,** 106 (1989).
4. K.-V. Peinemann and I. Pinnau, U.S. Pat. 4,746,333 (1988).
5. T. S. Chung, E. R. Kafchinski, and R. Vora, to appear.
6. I. Pinnau and W. J. Koros, *Ind. Eng. Chem. Res.*, **20,** 2234 (1991).
7. J. E. Cadotte, U.S. Pat. 4,277,344 (1981).
8. K. Kimmerle, T. Hofmann, and H. Strathmann, *J. Membr. Sci.*, **61,** 1 (1991).
9. W. Gudernatsch, Th. Menzel, and H. Strathmann, *J. Membr. Sci.*, **61,** 19 (1991).
10. I. Pinnau, J. G. Wijmans, I. Blume, T. Kuroda, and K.-V. Peinemann, *J. Membr. Sci.*, **37,** 81 (1988).
11. M. Niwa, H. Ohya, Y. Tanaka, N. Yoshikawa, K. Matsumoto, and Y. Negishi, *J. Membr. Sci.*, **39,** 301 (1988).
12. J. S. Chiou and D. R. Paul, *J. Appl. Polym. Sci.*, **3,** 2935 (1987).
13. Y. Maeda and D. R. Paul, *Polymer,* **26,** 2055 (1985).
14. T. Kajiyama, S. Washizu, and Y. Ohmori, *J. Membr. Sci.*, **39,** 73 (1985).
15. M. Pasternak, C. R. Bartels, J. Reale, Jr., and V. M. Shah, U.S. Pat. 4,960,519 (1990).
16. I. Cabasso and A. P. Tamvakis, *J. Appl. Polym. Sci.*, **23,** 1509 (1979).
17. B. Bikson, E. Miller, and J. K. Nelson, U.S. Pat. 4,881,954 (1989).
18. T. C. Golden, M. B. Rao, and S. Sircar, U.S. Pat. 5,104,425 (1992).
19. M. Anand, C. A. Costello, and K. Campbell, U.S. Pat. 5,013,338 (1991).
20. M. Anand, P. S. Puri, K. Campbell, and C. A. Costello, U.S. Pat. 5,073,175 (1991).
21. H. Bruschke, U.S. Pat. 4,755,299 (1988).
22. S. Takao, U.S. Pat. 4,409,162 (1983).
23. W. Albrecht, P. Klug, W. Makschin, T. Weigel, V. Grobe, D. Paul, M. Holtz, and K. Muller, World Pat. 89-069193/10 (1989).
24. T. H. Kim, W. J. Koros, G. R. Husk, and K. C. O'Brien, *J. Membr. Sci.*, **37,** 45 (1988).
25. L. M. Robeson, *J. Membr. Sci.*, **62,** 165 (1991).
26. T. S. Chung, E. R. Kafchinski, and P. Foley, *J. Membr. Sci.*, **75,** 181 (1992).
27. R. A. Hayes, U.S. Pat. 4,912,197 (1990).

Received August 11, 1993
Accepted November 9, 1993